Journal of Molecular Structure 1218 (2020) 128441

Contents lists available at ScienceDirect

Journal of Molecular Structure

journal homepage: http://www.elsevier.com/locate/molstruc

N-(4-bromobenzylidene)-2,3-dihydrobenzo[b][1,4]dioxin-6-amine: Synthesis, crystal structure, docking and *in-vitro* inhibition of PLA2

M.K. Hema [a], R.R. ArunRenganathan [b], S. Nanjundaswamy [c], C.S. Karthik [c], Yasser Hussein Issa Mohammed [d], Saad Alghamdi [e], N.K. Lokanath [a], V. Ravishankar Rai [b], S. Nagashree [c, *], P. Mallu [c, **]

[a] *Department of Studies in Physics, University of Mysore, Manasagangotri, Mysuru, 570 006, Karnataka, India*
[b] *Department of Studies in Microbiology, University of Mysore, Manasagangotri, Mysuru, 570006, Karnataka, India*
[c] *Department of Chemistry, SJCE, JSS Science and Technology University, Mysuru, 570 006, Karnataka, India*
[d] *Department of Biochemistry, Faculty of Applied Science College, University of Hajjah, Yemen*
[e] *Laboratory Medicine Department, Faculty of Applied Medical Sciences, Umm Al-Qura University, Makkah, Saudi Arabia*

ARTICLE INFO

Article history:
Received 16 October 2019
Received in revised form
1 May 2020
Accepted 11 May 2020
Available online 26 May 2020

Keywords:
Docking
4-Bromobenzaldehyde
Anti-inflammatory activity
PLA2
Schiff base

ABSTRACT

The novel *N*-(4-bromobenzylidene)-2,3-dihydrobenzo[b][1,4]dioxin-6-amine compound is designed and subjected to structural studies, inhibition of sPLA2, and molecular docking. The compound was synthesized by condensation of 1,4-benzodioxan-6-amine and 4-bromobenzaldehyde and characterized by various spectral techniques. Single crystal X-ray diffraction analysis confirmed the 3D molecular structure and established the different intermolecular interactions responsible for the crystal structure stability. Further synthesized compound was evaluated for anti-inflammatory activity using sPLA2 inhibition by indirect hemolytic assay. The compound showed good inhibition against sPLA2 enzyme compared with standard diclofenac, which is validated by molecular docking with a −7.60 kcal/mol docking score.

1. Introduction

Phospholipase A2 (PLA2) is a phospholipases class which hydrolyze phospholipids, produces lysophospholipids and proinflammatory oxidized free fatty acids such as arachidonic acid (AA). When arachidonic acid released cyclooxygenases (COX-1 and COX-2), lipoxygenase (LOX) and forms eicosanoids, prostaglandins, and leukotrienes. PLA2 plays a vital role in the inflammation process [1]. The different types of PLA2 involve in various lipid signalling and inflammatory diseases [1]. These PLA2 enzymes are involved in rheumatoid arthritis, lung inflammation, multiple sclerosis, cardiovascular diseases, and atherosclerosis [2–4]. Regarding the development of potent and selective inhibitors, none of them have entered the market until now. Thus, there is a great interest in developing potent and selective PLA2 inhibitors, and some of them have entered clinical trials [5]. In particular, inhibitors of the PLA2 enzymes are potential new agents for the treatment of various inflammatory diseases. GIVA cPLA2 inhibitors are in the initial stage of rheumatoid arthritis in clinical studies, while inhibitors of GVIA iPLA2 are in the preclinical phase [6]. Apart from that, there are some novel selective inhibitors of sPLa2 are GK264, KH064, AZD2716, and indole-based inhibitors for example, varespladib, varespladib methyl, sPLA2-X inhibitor 1, 31, [7–10] are given in Fig. 1.

Compounds containing 1,4-benzodioxane moiety gained significant attention in medicinal and pharmaceutical applications due to various biological activities like anti-inflammatory [11,12], analgesic [13], antimicrobial [14,15], anticonvulsant [16], antitubercular [17], anticancer [18], antioxidant [19] and so forth. There are many structural scaffolds found in a variety of drugs. In view of these findings, we have attempted to synthesis a new 1,4-benzodioxane containing Schiff base compound for selective inhibition of PLA2 enzyme, and the structure was confirmed by a single X-ray diffractometer. From the *in-silico* method, inhibition of the

* Corresponding author.
** Corresponding author.
E-mail addresses: nagashrees@sjce.ac.in (S. Nagashree), drmallu66@gmail.com (P. Mallu).

https://doi.org/10.1016/j.molstruc.2020.128441
0022-2860/

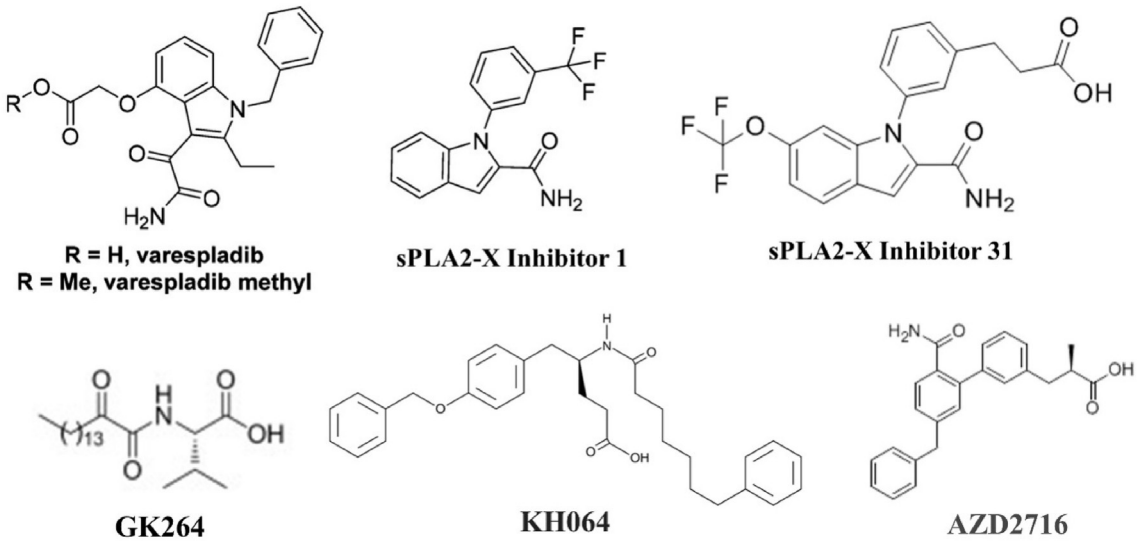

Fig. 1. Some of selective sPLA2 inhibitors.

PLA2 enzyme was confirmed and correlated with an *in-vitro* method.

2. Experimental

2.1. Materials and methods

All solvents and reagents were purchased from Merck and Sigma Aldrich Chemicals. The elemental analyses were obtained from PerkinElmer 2400 elemental analyzer. The FT-IR spectrum was recorded on Jasco FT-IR 4100 infrared spectrophotometer using KBr discs. LC/MSD Trap XCT obtained mass spectral data. The ^{1}H NMR spectra were recorded using Bruker DRX 400 spectrometer using DMSO-d_6 as solvent at 400 MHz and TMS as the internal standard.

2.2. Chemistry

Synthesis of *N*-(4-bromobenzylidene)-2,3-dihydrobenzo[b][1,4]dioxin-6-amine

Equimolar concentrations of 4-bromo benzaldehyde (0.1403 g) and 1, 4-benzodioxan-6-amine (0.1147 g) was dissolved in methanol and allowed to stir for about 8–10 h at room temperature, and a catalytic amount of concentrated sulfuric acid was added. The forward of the reaction was examined by thin-layer chromatography (TLC). After the reaction completion, the solvent and the product were separated in the vacuum pump and crystallized from methanol. Synthesis of 1,4-benzodioxan-6-amineSchiff bases is outlined in Scheme 1

FT-IR (KBr, cm^{-1}) ν: 3036 (Ar–H), 1632 (CH=N), 1510 (C=C), 552 (C–Br), 1118 (C–N), 1123 (C–O). ^{1}H NMR δ ppm: 8.39 (CH=N, s, 1H), 7.51 (Aromatic-H, d, 2H), 7.46 (Aromatic-H, d, 2H), 6.70 (Aromatic-H, d, 2H), 6.70 (Aromatic-H, s, 1H), 4.36 (CH_2, t, 4H). MS (ESI) *m/z*: 318.17. Anal.calcd. for $C_{15}H_{12}BrNO_2$ (in %): C-56.62, H-3.80, N-4.40. Found: C-56.75, H-3.92, N-4.65.

2.3. X-ray structure determination

Suitable brown colored rectangle-shaped single crystal of title compound was selected for data collection. X-ray intensity data were collected using RigakuXtaLAB mini CCD diffractometer with X-ray generator operating at 50 kV and 12 mA, Mo-Kα (λ = 0.71073 Å) radiation source, keeping the scan width of 0.5°, exposure time of 3 s, the sample to detector distance of 50 mm. A complete data set was processed using *CRYSTALCLEAR* [20]. The structures were solved using *SHELXS* structure solution program by direct methods and refined with the *SHELXL* [21] refinement package using least-squares minimization. The geometrical calculations were carried out using *PLATON* [22], and the diagrams were generated using *MERCURY* [23]. The crystal data and the structure refinement details for *N*-(4-bromobenzylidene)-2,3-dihydrobenzo[b][1,4]dioxin-6-amine are given in Table 1.

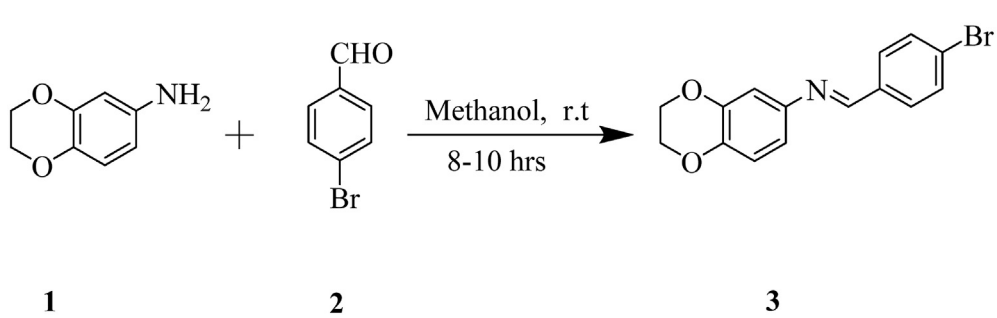

Scheme 1. Synthetic route of the title compound.

Table 1
Crystal data and structure refinement details.

Parameters	Data
CCDC deposit No.	1895716
Empirical formula	$C_{15}H_{12}BrNO_2$
Formula weight	318.16
Temperature (K)	293
Wavelength (Å)	0.71073
Crystal system, space group	Triclinic, $P\overline{1}$
Unit cell dimensions	
a	8.177(4) Å
b	8.377(4) Å
c	10.960(5) Å
α	72.899(8)°
β	69.480(8)
γ	89.743(7)
Volume Å^3	667.9(6)
Z	2
Density(calculated) (Mg m^{-3})	1.582
Absorption coefficient (mm^{-1})	3.074
F_{000}	320
θ range for data collection	3.49°−27.48°
Index ranges	$-10 \leq h \leq 8$
	$-10 \leq k \leq 10$
	$-14 \leq l \leq 13$
Reflections collected	3615
Independent reflections	2865 [$R_{int} = 0.0249$]
Absorption correction	Multi-scan
Refinement method	Full matrix least-squares on F^2
Data/restraints/parameters	2865/0/173
Goodness-of-fit on F^2	1.016
Final [$I > 2\sigma(I)$]	$R1 = 0.0582$, w$R2 = 0.1373$
R indices (all data)	$R1 = 0.1040$, w$R2 = 0.1610$
Extinction coefficient	0.011(3)
Largest diff. peak and hole	0.520 and −0.454 eÅ^{-3}

2.4. Hirshfeld surface analysis

Hirshfeld surface analysis was carried out using *Crystal Explorer 3.1* [24] to analyze intermolecular interactions, such as hydrogen bonds and the weaker C−H...π and π...π interaction. Three-dimensional d_{norm} pictures of title compound are generated where identical colored regions characterize the close intermolecular contacts. The quantities de and di describe the distance from the nearest atoms outside and inside to the Hirshfeld surface, respectively. The close intermolecular contacts are summarized in a fingerprint plot.

2.5. Anti-inflammatory activity

The protein concentration in the venom was calculated, using bovine serum albumin (BSA) fraction (0−75 μg). A semi-quantitative indirect haemolytic assay was employed by a previous report [12]. Briefly, egg yolk packed human erythrocytes, and phosphate buffer saline was mixed (1:1:8 V/V). This suspension (1 mL) was incubated with 60 μg enzyme for 10 min at 37 °C. The amount of haemoglobin released in the supernatant was measured at 540 nm. The assay was also carried out in the concentrations range (0−200 μg/mL) of the synthesized compound. The lysis of erythrocytes by adding 9 mL of phosphate buffer saline to the test tube containing enzyme and inhibitor without the compound was taken as 100%.

2.6. In-silico studies: molecular docking

The molecular docking analysis was carried out by using MGL tools 1.5.6 to understand the interactions of the synthesized ligand toward target PLA2 protein, [25,26] with *AutoDock Vina* [27]. The three-dimensional Crystallographic structures of *Daboiarusselii* Type IIA secretory phospholipase A2 (PLA2) complex with diclofenac (PDB ID: 2B17) were retrieved in pdb format from the Protein Data Bank. The protein was freed from inbound ligand (diclofenac) by *Discovery Studio 2019 Client visualizer*. Then the addition of polar hydrogen atoms to the protein and ligand preparation was employed by the *AutoDock* Tools (ADT). The grid box was selected for proteins centered at the crystal structure with the size at 51.468, 35.07, 0.01, for X, Y, Z respectively. Molecular docking simulations were performed with *AutoDock Vina* implemented through the shell script provided by developers [28]. The binding affinity of ligand was observed by kcal/mole as a unit for a negative score. *Biovia Discovery Studio* software was utilized for the visualization and interpretation of the obtained docking results of PLA2 ligand interaction.

3. Results and discussion

3.1. Chemistry

The chemical structure of the synthesized compound is shown in the scheme. Different spectral studies confirmed the synthesized compound. Theoretically calculated values and experimentally determined values of elemental analysis lies within ± 0.4%.

The FT-IR spectrum was recorded using KBr pellets in the range of 4000 - 400 cm^{-1}. The absence of NH_2, C═O, and presence of −CH═N- absorption bands in the IR spectra confirmed the formation of new compounds. The aromatic C−H stretching vibrations appear around 3036 cm^{-1} in the synthesized compound. The azomethine (C═N) stretching vibrations appear around 1632 cm^{-1} as medium or strong absorption bands in the synthesized compound. The strong bands at 552 cm^{-1} assigned to the C−Br stretch. The proton spectral data of the key intermediate, compound shows resonance at δ 5.61 ppm (s, 2H, $-NH_2$). But in the spectra of the synthesized compound, the azomethine proton −CH═N- showed the resonance at δ 8.39 ppm, which confirmed the identity of the product. The mass spectra of the synthesized compounds showed a molecular ion peak at m/z 317.0043, which is in agreement with the molecular formula $C_{15}H_{12}BrNO_2$ (Fig. 2).

3.2. Single crystal X-ray diffraction

Molecular structure of the *N*-(4-bromobenzylidene)-2,3-dihydrobenzo[b] [1,4]dioxin-6-amine is investigated by single-crystal X-ray diffraction method. The X-ray structural analysis revealed that the synthesized compound crystallized in centro-symmetric space group $P\overline{1}$ with two molecules per unit cell. The ORTEP diagram with the numbering scheme of the title compound is shown in Fig. 3a. The molecule is non linear and it is observed that nitrogen atom (N1) of the Schiff base moiety is slightly twisted about torsion angle of 163.02° (C7−N1−C8−C13) which leads to the non-planarity between bromobenzene and benzodioxane moieties, which is evidenced by the 16.83° dihedral angle between the planes Br−C1−C2−C3−C4−C5−C6−C7 and C8−C9−C10−C11−C12−C13−O1−O2 Fig. 3b. The valence angles of bromobenzene ring range 117.66−121.66° and the same of a

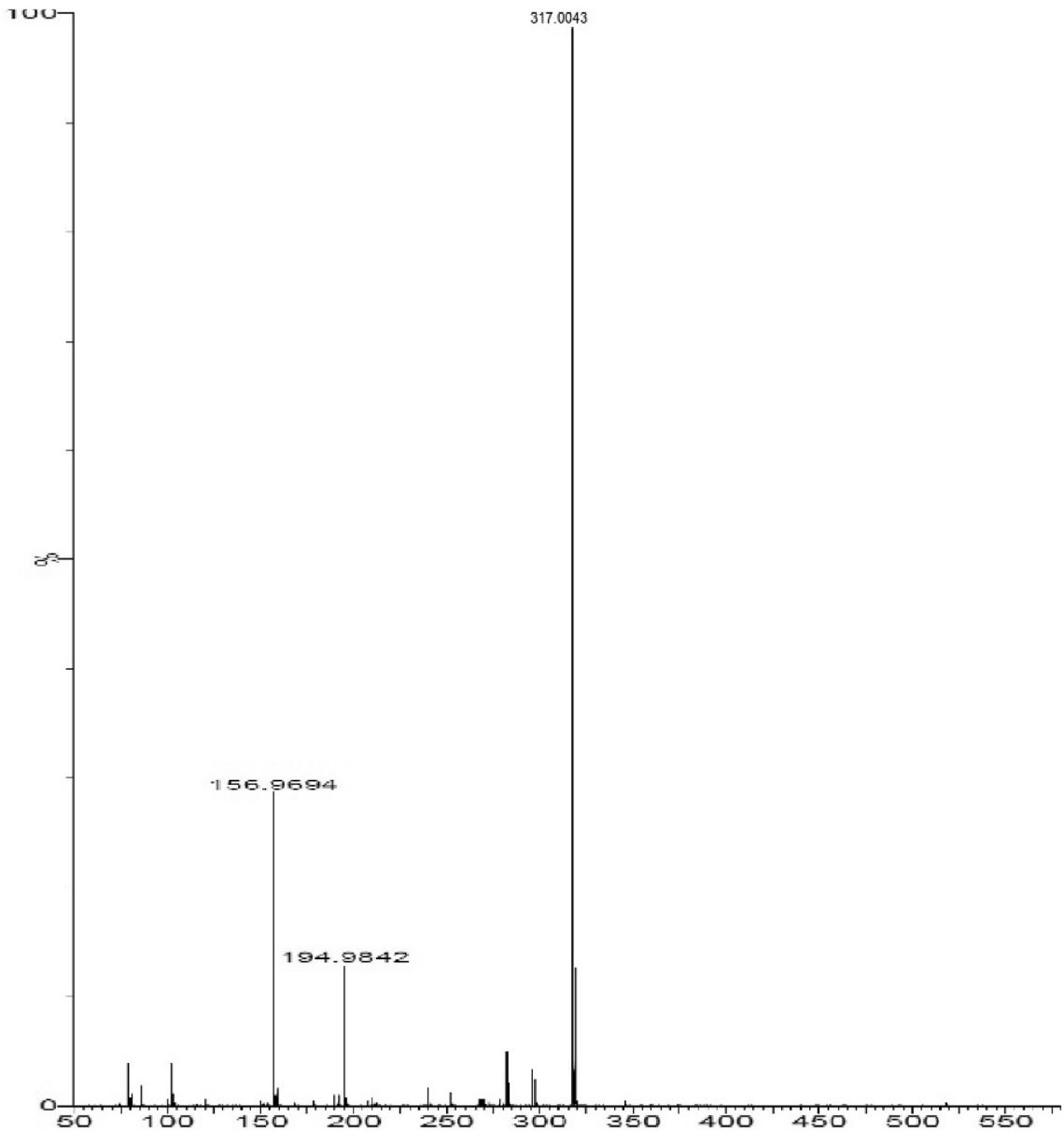

Fig. 2. Mass spectra of compound 3.

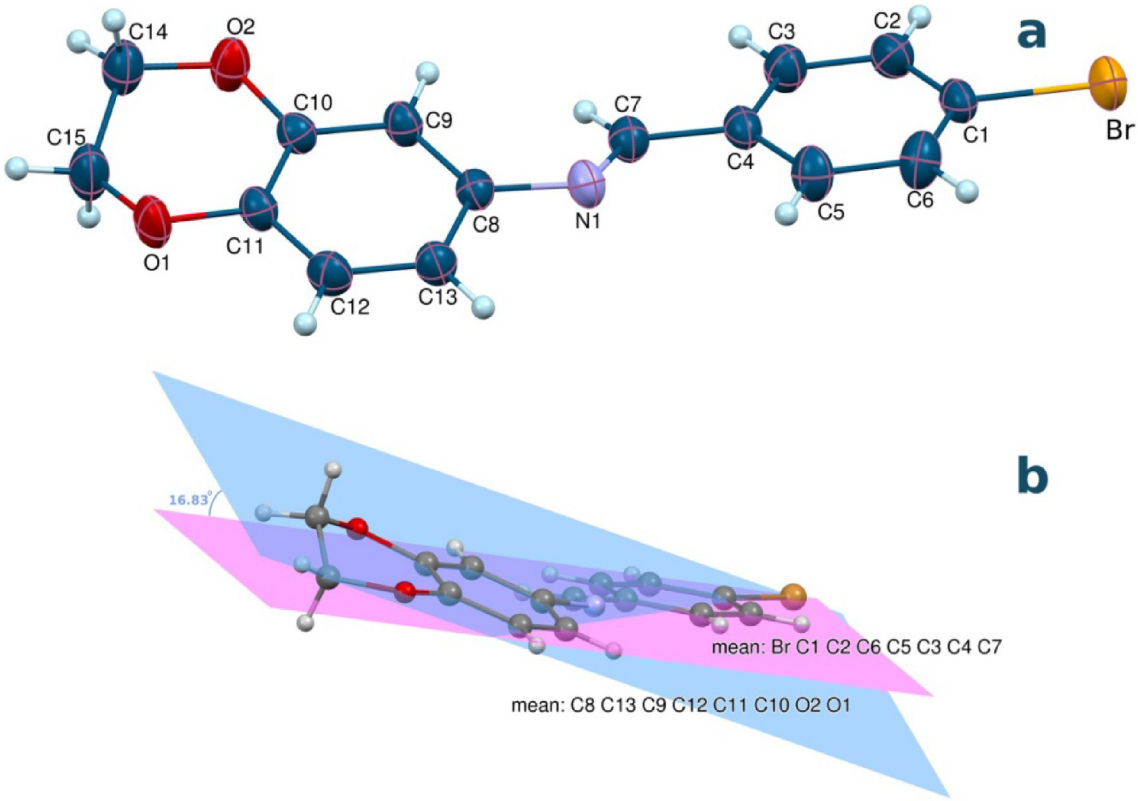

Fig. 3. (a) ORTEP diagram with thermal ellipsoids are drawn at 50% probability. and (b) Non-linearity representation of the title compound.

Table 2
Selected bond lengths (Å) and bond angles (°) of the synthesized compound.

Bond lengths (Å)				Bond angles (°)			
Atoms	Length	Atoms	Length	Atoms	Angle	Atoms	Angle
Br–C1	1.908(5)	C4–C5	1.386(7)	C11–O1–C15	112.2(4)	N1–C8–C9	124.6(4)
O1–C11	1.374(6)	C4–C7	1.456(7)	C10–O2–C14	115.4(4)	N1–C8–C13	117.3(4)
O1–C15	1.417(7)	C5–C6	1.383(8)	C7–N1–C8	122.4(4)	C9–C8–C13	118.0(4)
O2–C10	1.379(6)	C8–C9	1.390(7)	Br–C1–C2	119.9(4)	C8–C9–C10	120.7(4)
O2–C14	1.415(7)	C8–C13	1.380(7)	Br–C1–C6	118.6(4)	O2–C10–C9	117.6(4)
N1–C7	1.249(7)	C9–C10	1.369(7)	C2–C1–C6	121.5(5)	O2–C10–C11	121.6(4)
N1–C8	1.416(6)	C10–C11	1.374(6)	C1–C2–C3	119.0(5)	C9–C10–C11	120.8(5)
C1–C2	1.364(8)	C11–C12	1.381(7)	C2–C3–C4	121.7(5)	O1–C11–C10	122.4(4)
C1–C6	1.356(8)	C12–C13	1.370(7)	C4–C5–C6	120.5(5)	C8–C13–C12	121.2(5)
C2–C3	1.368(8)	C14–C15	1.440(9)	C1–C6–C5	119.7(5)	O2–C14–C15	112.5(5)
C3–C4	1.391(7)			N1–C7–C4	123.7(5)	O1–C15–C14	114.5(5)

benzene ring attached to the dioxane range from 118.00 to 121.24° but the C14 and C15 atoms of dioxane ring deviate by 0.221 and 0.402 Å respectively, from the benzodioxane least-square plane. The inter-ring (1.368–1.39 Å) and C=N (1.249 Å) distances are compared well with values observed for bromobenzene Schiff base derivatives [29]. Bond lengths, bond angles, and torsion angles are given in Tables 2–4, respectively.

The molecular structure of the title compound is stabilized by several intermolecular interactions such as inter and intramolecular hydrogen bond interaction, C–H...π, and π... π interactions. Intermolecular hydrogen bond interaction H11A...Br with a donor-acceptor distance of 2.88 Å respectively, where D – H...A angle is 171° and the symmetry code is −2+x,-1+y,1+z combines the four adjacent molecules to form supramolecular synthon $R_4^4(16)$ (Fig. 4). Along with this interaction, C2 of bromobenzene ring interacts with O2 of dioxane through its hydrogen (H7) atom with a donor-acceptor distance of 2.71 Å, which leads to the formation of supramolecular synthon $R_2^2(20)$ (Fig. 4) along *a* and *c* axis. Interestingly, these two interactions join together to promote the molecules to diagonally arranged rhomboidal chain packing along the crystallographic *bc* plane. In addition to these interactions, C14 atom is involved in an intermolecular interaction with the π system of dioxane attached benzene ring C8/C9/C10/C11/C12/C3 (C14–H14B…..Cg3, where Cg3 is the centroid of the ring, with a symmetry code -1-x,-y,2-z having C–Cg distance of 3.649(5) Å, C–H…Cg angle of 165°) of benzodioxane moiety, which is shown in the Fig. 4a. benzodioxane moiety plays a significant role in crystal packing via its intermolecular π….π stacking. The centroid of dioxane ring interacts with the same benzene ring of an adjacent molecule with Cg...Cg distance of 4.09 Å and the dihedral

Table 3
Torsion angles (°) of the synthesized compound.

Atoms	Angle	Atoms	Angle
C15–O1–C11–C10	16.6(6)	C3–C4–C7–N1	−174.0(5)
C15–O1–C11–C12	−163.8(5)	C5–C4–C7–N1	4.9(8)
C11–O1–C15–C14	−44.3(6)	C4–C5–C6–C1	0.3(9)
C14–O2–C10–C9	−171.6(4)	N1–C8–C9–C10	−178.5(4)
C14–O2–C10–C11	8.3(6)	C13–C8–C9–C10	−0.5(7)
C10–O2–C14–C15	−35.1(6)	N1–C8–C13–C12	179.3(4)
C8–N1–C7–C4	176.8(4)	C9–C8–C13–C12	1.2(7)
C7–N1–C8–C9	−19.0(7)	C8–C9–C10–O2	179.0(4)
C7–N1–C8–C13	163.1(5)	C8–C9–C10–C11	−0.9(7)
Br–C1–C2–C3	−179.5(4)	O2–C10–C11–O1	1.5(6)
C6–C1–C2–C3	1.7(8)	O2–C10–C11–C12	−178.2(4)
Br–C1–C6–C5	179.8(4)	C9–C10–C11–O1	−178.6(4)
C2–C1–C6–C5	−1.4(9)	C9–C10–C11–C12	1.7(7)
C1–C2–C3–C4	−1.0(8)	O1–C11–C12–C13	179.3(4)
C2–C3–C4–C5	−0.1(7)	C10–C11–C12–C13	−1.0(7)
C2–C3–C4–C7	178.9(5)	C11–C12–C13–C8	−0.4(8)
C3–C4–C5–C6	0.4(8)	O2–C14–C15–O1	54.9(7)
C7–C4–C5–C6	−178.6(5)		

angle between planes of 15.12° (Fig. 5b).

3.3. Hirshfeld surface analysis

Three-dimensional Hirshfeld surfaces of the synthesized compound mapped on d_{norm} is shown in Fig. 6. Two dark red circular spots on the Hirshfeld surface evidence the hydrogen bonding interaction of type C15–H11A...Br. A relatively big red circle on the Hirshfeld surfaces mapped on d_e and shape index illustrate the C–H...pi interaction type C14–H14B…..Cg3 (Fig. 6b). H···H interactions (39.3%) appear in the middle of scattered points in the 2D fingerprint plot have a significant contribution to the total Hirshfeld surfaces. Br···H interactions viewed as sharp wings in the upper and lower corner of the 2D fingerprint plot comprised of 15.8%, C···H/H···C interactions appear as two broad spikes in the lower middle of the 2D fingerprint plot (14.9%) and H···O/H···O intermolecular interactions which are reflected by the two sharp spikes in the middle of the 2D fingerprint plot comprised of 12.3% have relatively significant contribute onto the total Hirshfeld surfaces. Apart from these interactions, some minor interactions are also observed, which are seen in Fig. 7.

3.4. Biology

3.4.1. In-vitro PLA2 assay

PLA2 is an enzyme that catalyzes the release of free fatty acids, and it exhibits high specificity for membrane phospholipids containing arachidonic acid (AA). PLA2 is the primary AA provider for the cyclooxygenase (COX) and lipoxygenase (LOX) pathways and inflammatory mediators like eicosanoids or platelet-activating factor (PAF) to activate the inflammation pathway. PLA2 is the main component of the production eicosanoids, which are reasons for the various inflammatory diseases [30]. In the present work, the synthesized compound as an active anti-inflammatory molecule inhibits by the PLA2 enzyme. The extent inhibition of synthesized compound was studied by the dose dependent manner as a result, it showed up to 83% against sPLA2 shown in Fig. 8. The IC_{50} value of

Table 4
Docking results of synthesized compound and diclofenac.

Compound	Enzyme's binding site residue	Bond distance (Å)	Binding energy (Kcal/mol)
Synthesized compound	Leu2	4.29	−7.60
	Phe5	4.77	
	Cys45	5.83	
	Yyr28	3.74	
	Ala18	4.43	
	Ile19	5.10	
Diclofenac	Asp49	4.47	−7.80
	His48	2.44	
	Cys45	5.01	
	Cys29	5.89	
	Gly30	2.36	
	Phe5	4.83 & 4.90	
	Leu2	3.69 & 4.45	
	Ala18	5.03 &3.65	
	Ile19	5.27	

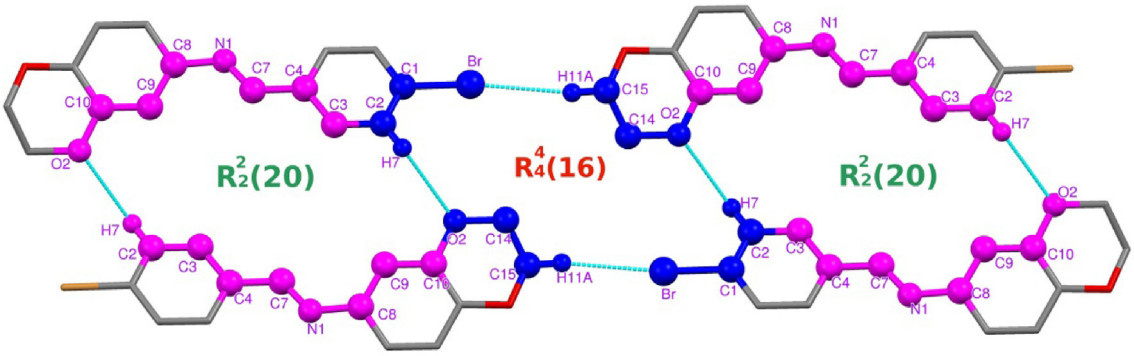

Fig. 4. Supramolecular synthons of the synthesized compound formed by intermolecular interactions between adjacent molecules.

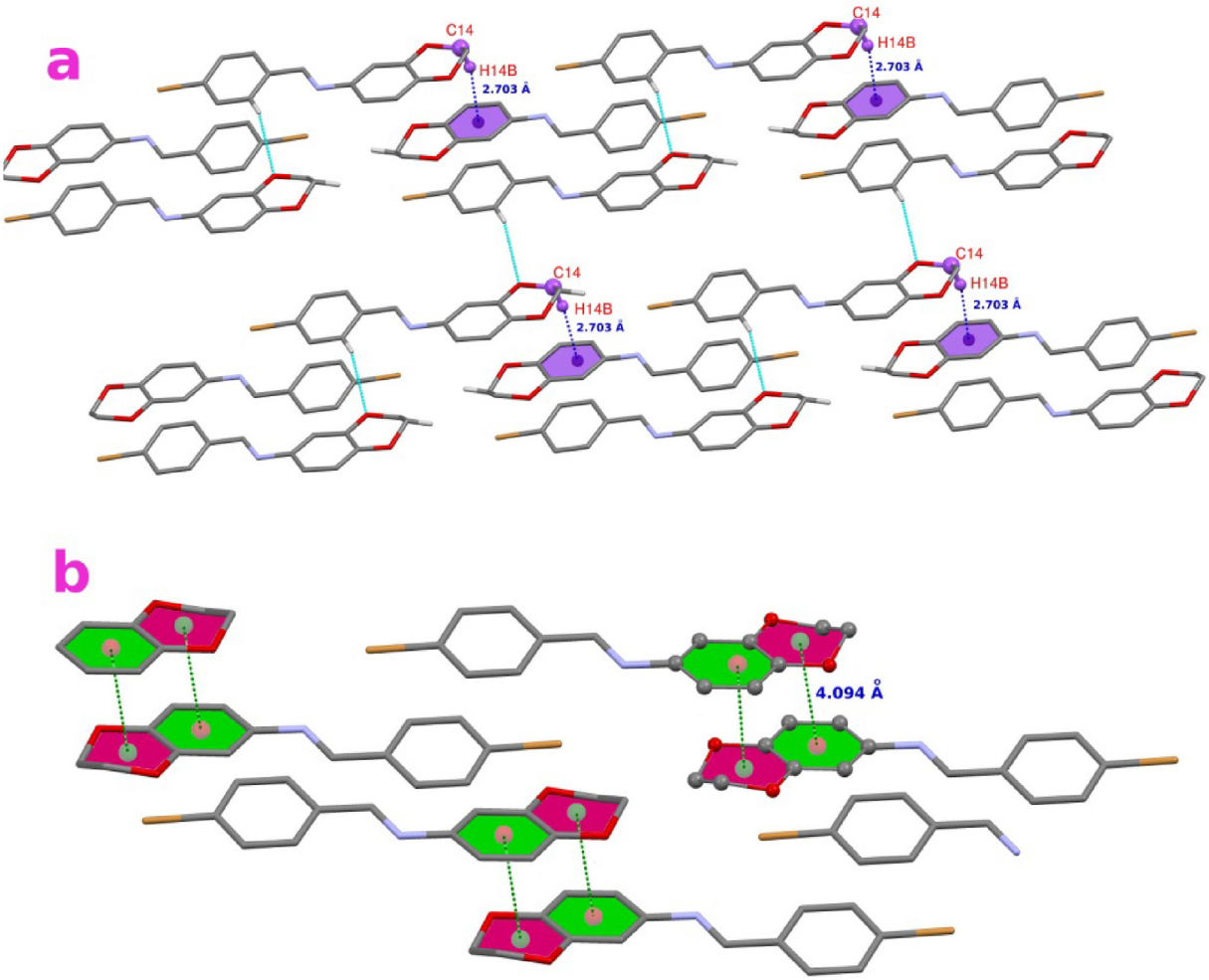

Fig. 5. (a) C–H...Cg and Cg...Cg interactions between adjacent molecules of the synthesized compound.

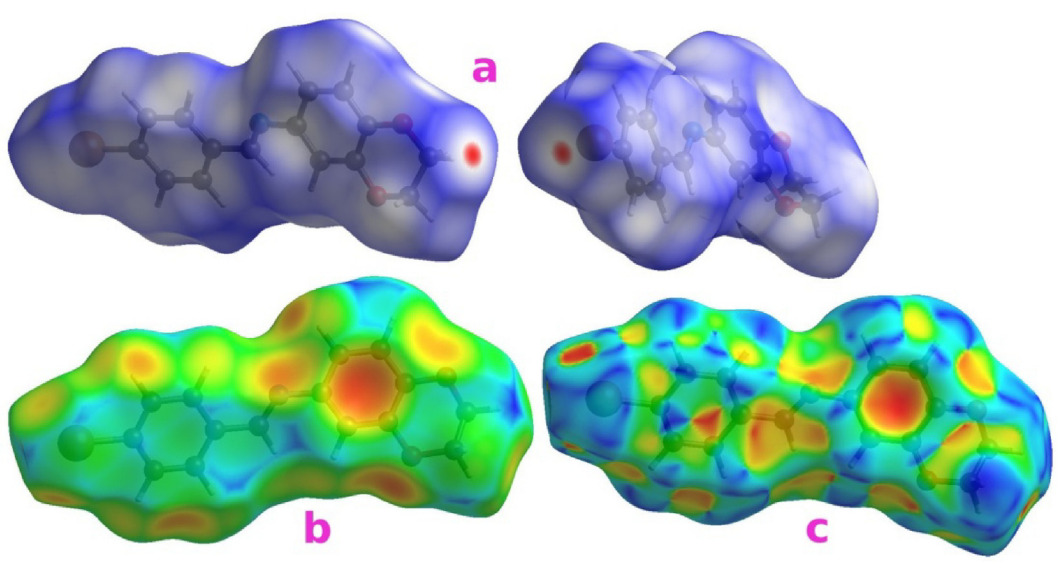

Fig. 6. 3D Hirshfeld surfaces mapped on (a) d_{norm}, (b) d_e and (c) shape index.

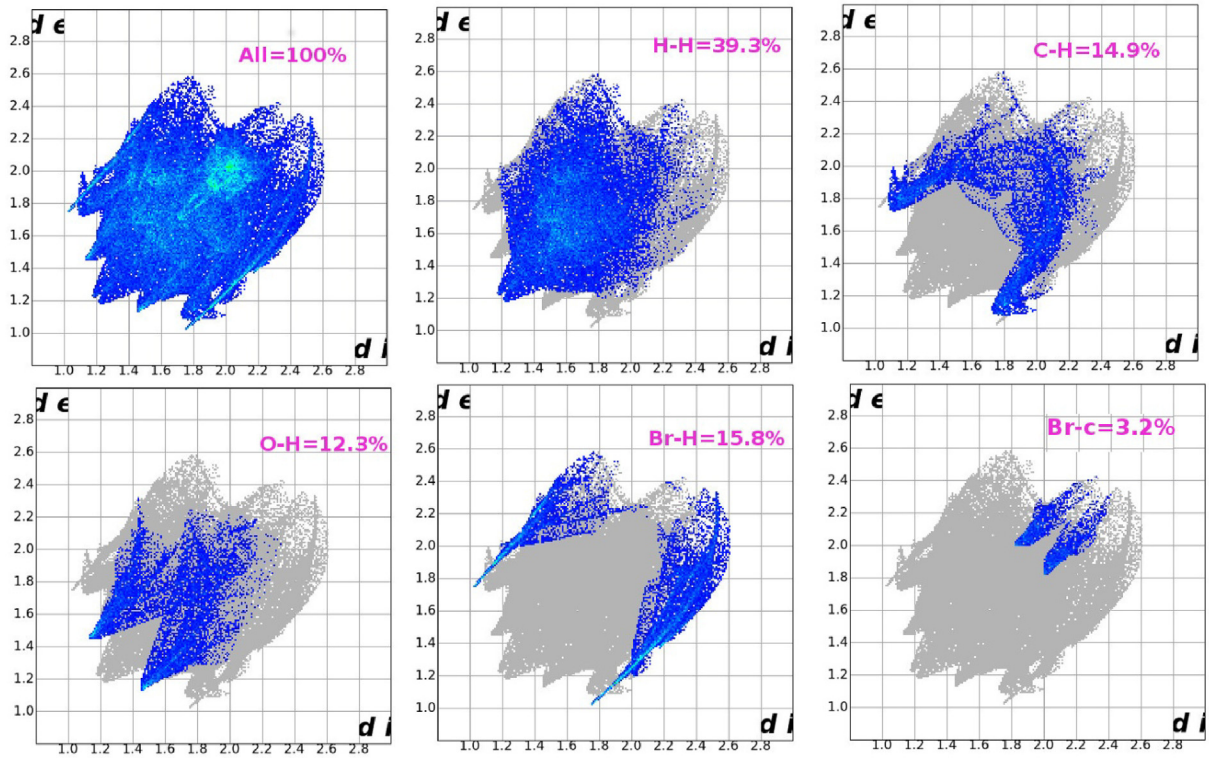

Fig. 7. 2D fingerprint plots of the synthesized compound.

the compound is 79 μg against the enzyme sPLA2 as compared to that of the standard drug diclofenac, having inhibitory action at 68 μg. The synthesized compound exhibited significant action against sPLA2 activity due to the presence of benzodioxane ring and which is validated on molecular docking.

3.5. Molecular docking

To predict the molecular interactions of the synthesized compounds with the PLA2 enzyme, molecular docking studies were performed by MGL tools 1.5.6 with AutoDock Vina software. Molecular docking analysis revealed that synthesized compound had good binding affinity compared with the standard drug diclofenac. The binding affinity of the synthesized compound is −7.6 kcal/mol, and for diclofenac is −7.8 kcal/mol. Docking of the synthesized compounds with PLA2 binding site showed that excellent fitted with the receptor and interacted with Leu2, Phe5, Cys45, Tyr28, Ala18 and Ile19 amino acids and discussed in the Table 3 (Fig. 9). Whereas, diclofenac interacted with amino acids such as Asp49, His48, Cys45, Cys29, Gly30, Phe5, Leu2, Ala18 and Ile19 (Fig. 10).

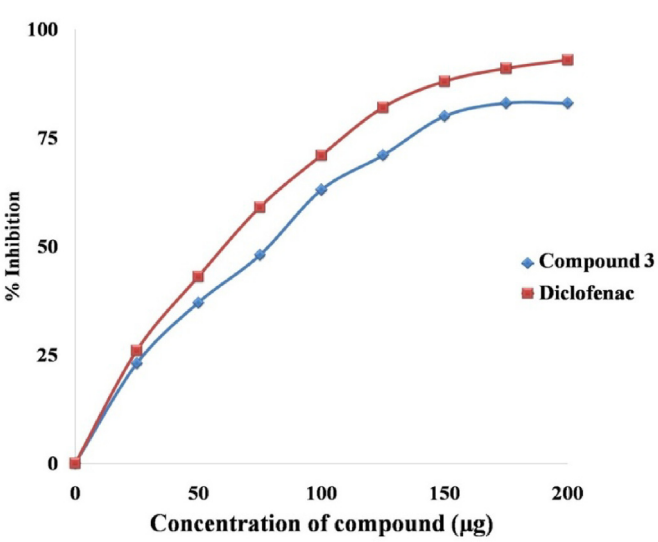

Fig. 8. Dose dependent inhibition of sPLA2 by synthesized compound.

4. Conclusion

In view of the significance of benzodioxane *N*-(4-bromobenzylidene)-2,3-dihydrobenzo[b][1,4]dioxin-6-amine compound was synthesized and characterized by various spectroscopic techniques. Further, the single-crystal structure was confirmed by the X-ray diffraction method. Intermolecular interactions responsible for the structural stability and formation of supramolecular synthons $R_2^2(20)$ and $R_4^4(16)$ are established. Hirshfeld surface analysis revealed that the H···H interactions (39.3%) contributes majorly to the total Hirshfeld surface. The synthesized compound evaluated for the PLA2 inhibition activity and validated with molecular docking.

Author contribution statements

CSK, NS and PM. conceived of the presented idea. NS did chemistry experimental, and CSK verified the analytical methods and data. ARR performed *in-vitro* biology, and SNS performed molecular docking. HMK developed the theory and performed the computations. PM, NKL, HEM and SA encouraged, supervised the findings of this work.

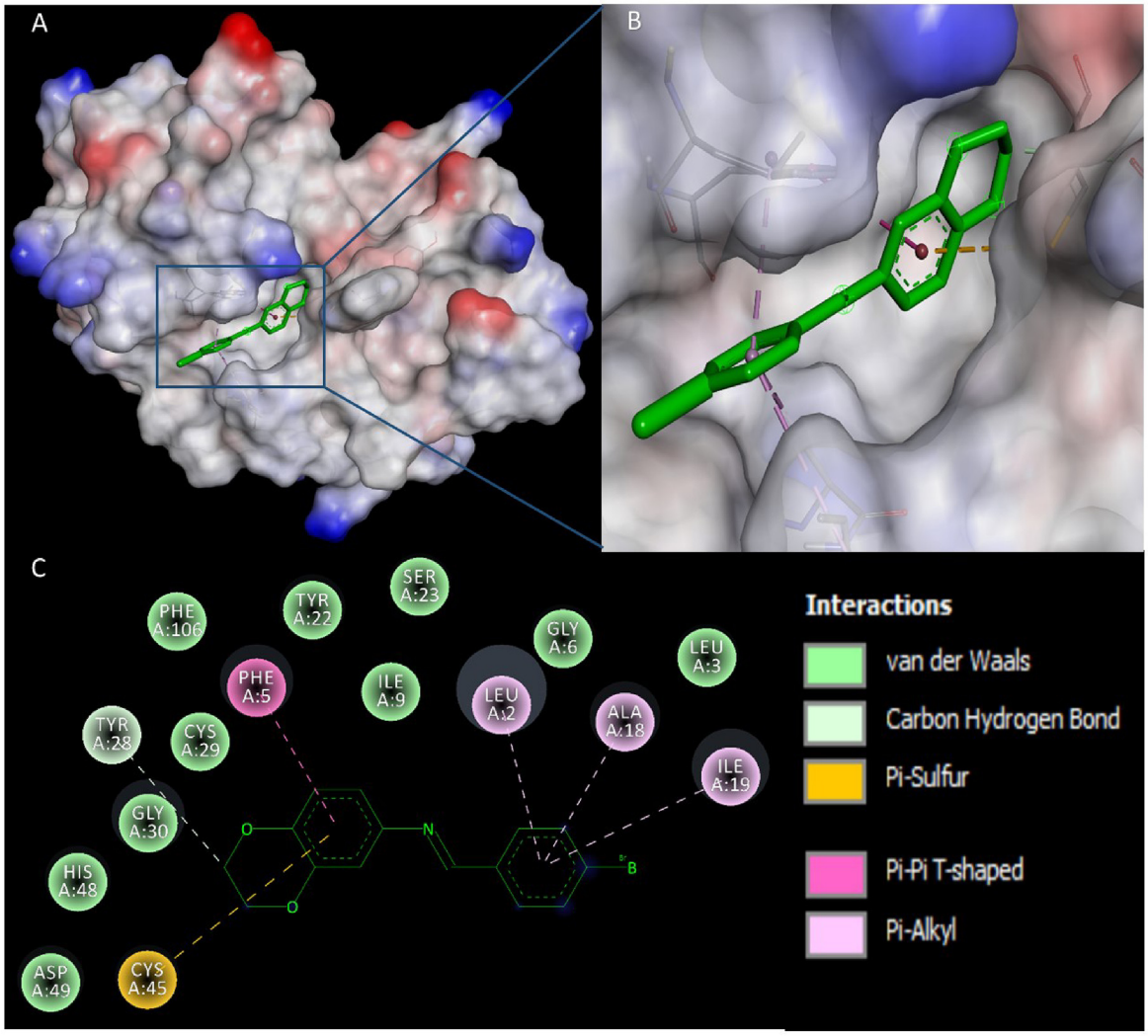

Fig. 9. 3D surface interaction of PLA2-Ligand complex (a), enlarged view of 3D surface pocket, and molecular interactions with active site amino acids in PLA2 (c).

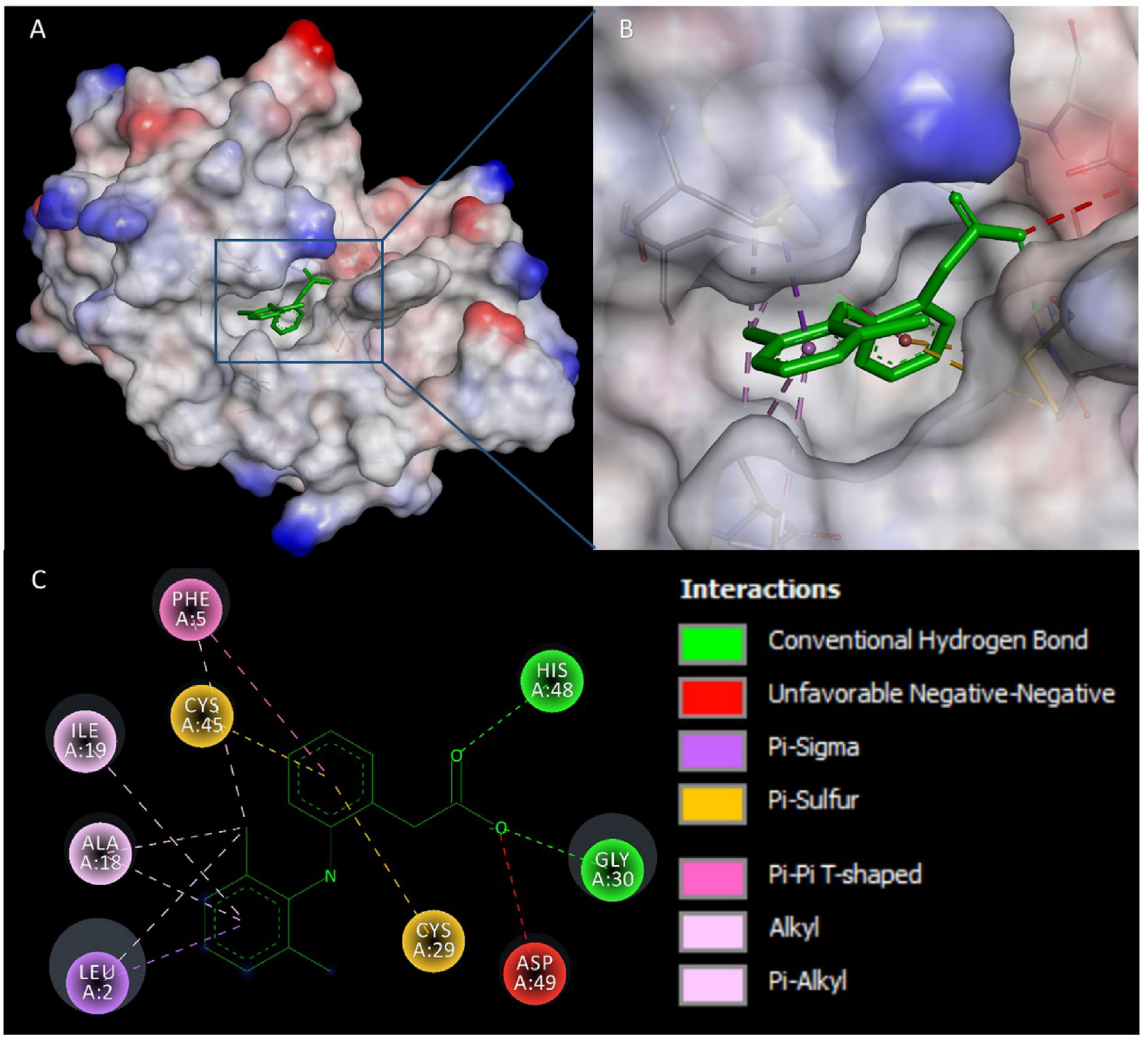

Fig. 10. 3D surface interaction of PLA2-Diclofenac complex (a), enlarged view of 3D surface pocket, and molecular interactions with active site amino acids in PLA2 (c).

Declaration of competing interest

The authors declare that they have no known competing financial interests or personal relationships that could have appeared to influence the work reported in this paper.

Acknowledgments

The authors are thankful to the Vision Group of Science and Technology (VGST), GRD-647/CISEE/2018, Dept. of IT, BT and S&T, Govt. of Karnataka, India for the financial support.

References

[1] A. Trotter, E. Anstadt, R.B. Clark, F. Nichols, A. Dwivedi, K. Aung, J.L. Cervantes, The role of phospholipase A2 in multiple Sclerosis: a systematic review and meta-analysis, Multiple sclerosis and related disorders 27 (2019) 206–213.
[2] A.O. Akinkuolie, P.R. Lawler, A.Y. Chu, M. Caulfield, J. Mu, B. Ding, F. Nyberg, R.J. Glynn, P.M. Ridker, E. Hurt-Camejo, D.I. Chasman, Group IIA secretory phospholipase A2, vascular inflammation, and incident cardiovascular disease: an analysis from the JUPITER trial, Arterioscler. Thromb. Vasc. Biol. 39 (6) (2019) 1182–1190.
[3] S.R. Robert, H.C. Eva, Phospholipase A2 enzymes and the risk of atherosclerosis, Eur. Heart J. 33 (2012) 2899–2909.
[4] V. Chiurchiù, A. Leuti, M. Maccarrone, Bioactive lipids and chronic inflammation: managing the fire within, Front. Immunol. 9 (2018) 38.
[5] A. Nikolaou, M.G. Kokotou, S. Vasilakaki, G. Kokotos, Small-molecule inhibitors as potential therapeutics and as tools to understand the role of phospholipases A2, BiochimicaetBiophysicaActa (BBA)-Molecular and Cell Biology of Lipids 1864 (6) (2019) 941–956.
[6] A. Psarra, M.G. Kokotou, G. Galiatsatou, V.D. Mouchlis, E.A. Dennis, G. Kokotos, Highly potent 2-oxoester inhibitors of cytosolic phospholipase A2 (GIVA cPLA2), ACS Omega 3 (8) (2018) 8843–8853.
[7] F. Giordanetto, D. Pettersen, I. Starke, P. Nordberg, M. Dahlström, L. Knerr, N. Selmi, B. Rosengren, L.O. Larsson, J. Sandmark, M. Castaldo, Discovery of AZD2716: a novel secreted phospholipase A2 (sPLA2) inhibitor for the treatment of coronary artery disease, ACS Med. Chem. Lett. 7 (10) (2016) 884–889.
[8] S. Vasilakaki, E. Barbayianni, G. Leonis, M.G. Papadopoulos, T. Mavromoustakos, M.H. Gelb, G. Kokotos, Development of a potent 2-oxoamide inhibitor of secreted phospholipase A2 guided by molecular docking calculations and molecular dynamics simulations, Bioorg. Med. Chem. 24 (8) (2016) 1683–1695.
[9] R.D. Dillard, N.J. Bach, S.E. Draheim, D.R. Berry, D.G. Carlson, N.Y. Chirgadze, D.K. Clawson, L.W. Hartley, L.M. Johnson, N.D. Jones, E.R. McKinney, Indole inhibitors of human nonpancreatic secretory phospholipase A2. 1. Indole-3-acetamides, J. Med. Chem. 39 (26) (1996) 5119–5136.
[10] L. Knerr, F. Giordanetto, P. Nordberg, D. Pettersen, N. Selmi, H.G. Beisel, H. de la Motte, T. Olsson, T.D. Perkins, M. Herslof, Å. Mansson, Discovery of a series of indole-2 carboxamides as selective secreted phospholipase A2 type X (sPLA2-X) inhibitors, ACS Med. Chem. Lett. 9 (7) (2018) 594–599.
[11] W.M. Wang, C. Wu, H.Z. Jin, Exosomes in chronic inflammatory skin diseases and skin tumors, Exp. Dermatol. 28 (3) (2019) 213–218.
[12] C.S. Karthik, H.M. Manukumar, A.P. Ananda, S. Nagashree, K.P. Rakesh, L. Mallesha, H.L. Qin, S. Umesha, P. Mallu, N.B. Krishnamurthy, Synthesis of novel benzodioxane midst piperazine moiety decorated chitosan silver nanoparticle against biohazard pathogens and as potential anti-inflammatory candidate: a molecular docking studies, Int. J. Biol. Macromol. 108 (2018) 489–502.

[13] C.S. Karthik, H.M. Manukumar, S. Sandeep, B.L. Sudarshan, S. Nagashree, L. Mallesha, K.P. Rakesh, K.R. Sanjay, P. Mallu, H.L. Qin, Development of piperazine-1-carbothioamide chitosan silver nanoparticles (P1C-Tit* CAgNPs) as a promising anti-inflammatory candidate: a molecular docking validation, MedChemComm 9 (4) (2018) 713–724.
[14] C.F. Huebner, Ciba-Geigy Corp, Analgesic and neuraleptic 2-piperidinoalkyl-1, 4-benzodioxans, U.S. Patent 4 (1979) 781, 140.
[15] L. Mallesha, K.N. Mohana, Synthesis, antimicrobial and antioxidant activities of 1-(1,4-benzodioxane-2-carbonyl) piperazine derivatives, Eur. J. Chem. 2 (2) (2011) 193–199.
[16] H.Y. Liu, T.R. Wang, G.H. Sheng, J. Qin, J. Sun, Synthesis, biological evaluation, and molecular docking of 1, 4-benzodioxan derivatives as potential antibacterial agents, Russ. J. Gen. Chem. 88 (12) (2018) 2601–2610.
[17] D.F. McComsey, V.L. Smith-Swintosky, M.H. Parker, D.E. Brenneman, E. Malatynska, H.S. White, B.D. Klein, K.S. Wilcox, M.E. Milewski, M. Herb, M.F. Finley, Novel, broad-spectrum anticonvulsants containing a sulfamide group: pharmacological properties of (S)-N-[(6-chloro-2, 3-dihydrobenzo [1,4] dioxin-2-yl) methyl] sulfamide (JNJ-26489112), J. Med. Chem. 56 (22) (2013) 9019–9030.
[18] H. Khalilullah, M. J Ahsan, M. Hedaitullah, S. Khan, B. Ahmed, 1, 3, 4-oxadiazole: a biologically active scaffold, Mini Rev. Med. Chem. 12 (8) (2012) 789–801.
[19] S. Wang, H.Y. Liu, R.F. Xu, J. Sun, Synthesis, biological evaluation, and molecular docking studies of diacylhydrazine derivatives possessing 1, 4-benzodioxan moiety as potential anticancer agents, Russ. J. Gen. Chem. 87 (11) (2017) 2671–2677.
[20] A. Czompa, Z. Dinya, S. Antus, Z. Varga, Synthesis and antioxidant activity of flavanoid derivatives containing a 1, 4-benzodioxane moiety, Arch. Pharmazie: An International Journal Pharmaceutical and Medicinal Chemistry 333 (6) (2000) 175–180.
[21] CrystalClear-Sm Expert 2011. Rigaku Corporation, Tokyo, Japan.
[22] G.M. Sheldrick, A short history of SHELXL, ActaCrystallogr A Found Adv 64 (1) (2008) 112–122.
[23] A.L. Spek, Structure validation in chemical crystallography, ActaCrystallogr D StructBiol 65 (2) (2009) 148–155.
[24] Mercury, Programme for Crystal Structure Visualization and Investigation of Crystal Structure *(V 3.8)*, Cambridge Crystallographic Data Centre, United Kingdom, 2017.
[25] S.K. Wolff, D.J. Grimwood, J.J. McKinnon, M.J. Turner, D. Jayatilaka, M.A. Spackman, CrystalExplorer, Uni. West. Aust., 2012, Version 3.0.
[26] R. Huey, G.M. Morris, A.J. Olson, D.S. Goodsell, A semiempirical free energy force field with charge-based desolvation, J. Comput. Chem. 28 (6) (2007) 1145–1152.
[27] G.M. Morris, D.S. Goodsell, R.S. Halliday, R.H. Huey, RK & Olson, AJ Automated docking using a Lamarckian genetic algorithm and an empirical binding free energy function, J. Comput. Chem. 19 (14) (1999) 1639–1662.
[28] O. Trott, A.J. Olson, AutoDock Vina: improving the speed and accuracy of docking with a new scoring function, efficient optimization, and multi-threading, J. Comput. Chem. 31 (2) (2010) 455–461.
[29] J.F.N. Batista, J.W. Cruz, A.C. Doriguetto, C. Torres, E.T. de Almeida, I. Camps, Synthesis, characterization and theoretical study in gaseous and solid phases of the imine 4-Acetyl-N-(4-methoxybenzylidene)aniline, J. Mol. Struct. 1147 (2017) 300–309, https://doi.org/10.1016/j.molstruc.2017.06.062.
[30] V.D. Mouchlis, D. Limnios, M.G. Kokotou, E. Barbayianni, G. Kokotos, J.A. McCammon, E.A. Dennis, Development of potent and selective inhibitors for group VIA calcium-independent phospholipase A2 guided by molecular dynamics and structure–activity relationships, J. Med. Chem. 59 (9) (2016) 4403–4414, https://doi.org/10.1021/acs.jmedchem.6b00377.